Electronic structure of Ni and Mo silicides investigated by x-ray emission spectroscopy and density functional theory

Ignace Jarrige,[*] Nathalie Capron, and Philippe Jonnard

LCPMR, UPMC Univ Paris 06, F-75005 Paris, France and UMR7614, Laboratoire de Chimie Physique-Matière et Rayonnement, CNRS,
11 rue Pierre et Marie Curie, 75231 Paris Cedex 05, France

We report a combined study of the electronic structure of $NiSi_2$, Ni_2Si, $MoSi_2$, and Mo_5Si_3 using x-ray emission spectroscopy and density functional theory. The local and partial metal d and Si p and sd densities of states (DOSs) are obtained for the four compounds both experimentally and theoretically. This allows refined insight into the Si-metal bonding interaction, shown to be determined by a competition between the effects of the lattice structure and of the spatial extent of the metal d wave function. The latter effect is found to prevail for all four compounds, based on the prominent Si-Mo pd hybridization found in the DOS of $MoSi_2$ and Mo_5Si_3 and the dominant Ni-Ni dd interaction observed in the electronic structure of $NiSi_2$ and Ni_2Si.

PACS number(s): 78.70.En, 71.20.−b

I. INTRODUCTION

For the last three decades, technological applications have aroused an increasing interest in transition-metal silicides. Owing to their easy production, low resistivity and thermal and mechanical stability, these systems have been extensively used in opto- and microelectronics.[1,2] Nickel silicides are promising candidates as contact materials in submicron complementary metal oxide semiconductor devices.[3,4] Refractory $MoSi_2$-based composite materials provide an effective coating for devices submitted to high temperatures such as furnaces or aircraft engines.[5] Most of the remarkable properties of metal silicides are arguably related to their electronic structure, and accordingly a wealth of studies have been reported on the electronic (and bonding) properties of these systems. However, there is a lack of comprehensive studies that include the local (element specific) and partial (symmetry specific) densities of states (DOSs) for a series of compounds. Most of previously reported multicompound studies were limited to either the total[6–8] or local[9–11] DOS, and those reporting local and partial DOS were restricted to only one compound.[12–19]

Accordingly, some of the critical aspects of bonding in silicides have not been plainly interpreted so far, such as the effect of the spatial extent of the metal d wave function. Also, compared to disilicides, general trends in bonding across transition-metal-rich silicides have been given only little attention until now.

In this work, we investigate both experimentally and theoretically the local and partial DOS of near-noble $NiSi_2$ and Ni_2Si and refractory $MoSi_2$ and Mo_5Si_3 silicides. The choice of these compounds is based on the considerations that (i) bond lengths and numbers of neighboring atoms are comparable for the two disilicides and for the two metal-rich silicides, respectively, and (ii) late $3d$ metal Ni and early $4d$ metal Mo should have relatively contracted and extended d wave functions, respectively. This allows us to disentangle the effects of the bonding environment and of the spatial extension of the metal d wave function in the discussion, which is a necessary condition to distill out the pivotal elements of bonding in metal silicides.

Most of the joint experimental and theoretical studies on the metal silicides reported so far used x-ray photoelectron spectroscopy (XPS) for the experimental spectra of the occupied states,[6,19–24] therefore most often restricting the discussion to the total DOS. X-ray emission spectroscopy (XES), by virtue of its site and symmetry selectivities, emerged as a key technique in elucidating solid-state electronic structure.[25–28] A few studies combining calculated and XES spectra of metal silicides have been previously reported, but the XES data are limited to Si.[12,29,30] We take here a step forward and present a more complete set of XES data consisting of the metal d and the Si p and sd states, thus allowing a greater experimental insight into the bonding mechanisms.

After describing the computational and experimental methods in Secs. II and III, respectively, we examine the calculated local and partial densities and discuss the bonding properties in Sec. IV A. These bonding schemes are closely corroborated by the experimental spectra as discussed in Sec. IV B. We suggest that the spatial extent of the metal d wave function plays a key role in determining the Si-metal bonding, as the Si-metal hybridization is found stronger in the Mo compounds compared with their Ni analogs, irrespective of the bond lengths and numbers.

II. COMPUTATIONAL DETAILS

The electronic structure calculations were performed using the VASP (Vienna *Ab initio* Simulation Package) code,[31,32] which was previously applied successfully to the electronic structure of transition-metal aluminides[33,34] and sulphides.[35] The program solves the Kohn-Sham equations through a three-dimensionally periodic implementation, within the framework of the density functional theory. The wave functions of the valence electrons were expanded in a basis set of plane waves with kinetic energy smaller than a specified cutoff energy, 245 eV for the Mo compounds and 270 eV for the Ni compounds. The Hamiltonian is based on pseudopotentials derived according to projector-augmented-wave potentials.[36] Reciprocal-space integration over the Brillouin zone was approximated through a sampling at a finite num-

TABLE I. Crystal structures of the metal silicides.

Compound	Structure	Space group	a(Å) b(Å) c(Å)	Site
MoSi$_2$	C11$_b$	I4/mmm	3.202	Mo 2a
			3.202	Si 4e
			7.851	
Mo$_5$Si$_3$	D8$_m$	I4/mcm	9.643	Mo1 4b
			9.643	Mo2 16k
			4.910	Si1 4a
				Si2 8h
NiSi$_2$	C1	Fm$\bar{3}$m	5.406	Ni 4a
			5.406	Si 8c
			5.406	
Ni$_2$Si	C23	Pnma	5.000	Ni1 4c
			3.730	Ni2 4c
			7.040	Si 4c

ber of k points using the Monkhorst-Pack scheme.[37] The approximation for the exchange-correlation function used is the generalized gradient approximation (GGA) of Perdew *et al.*,[38] which accounts well for changes in the coordination number.

We used the experimental lattice parameters for the sake of comparison with the experiment.[39] These are indicated in Table I along with the crystal structures of the four metal silicides. The coordination number for an *average* atom, i.e., the coordination number summed over the different sites and normalized by the number of sites, is plotted in Fig. 1 for the four silicides as a function of distance for the three contributions metal-metal, metal-Si, and Si-Si. These respective bonding contributions and their expected effect on the DOS are discussed in the beginning of Sec. IV A.

When compared to the experiment, the local and partial DOS are successively convoluted with (i) a Lorentzian (Gaussian) function accounting for the instrumental function for the metal d and Si p (Si sd) states, (ii) a Lorentzian function which full width at half maximum is equal to the lifetime of the core hole in the initial state of the emission process, and (iii) a Lorentzian function of variable width reflecting the variation in the lifetime of the hole across the valence band in the final state of the emission process. The width varies from 0 at the top to 1 eV at the bottom of the valence band, proportional to the square of the binding energy within the valence band.[15]

III. EXPERIMENTAL DETAILS

The XES measurements were performed on a MoSi$_2$ single crystal, and on Mo$_5$Si$_3$, NiSi$_2$, and Ni$_2$Si high-purity ($\geq$99%) powders purchased from Alfa Aesar and Mateck and compacted into pellets. Based on the high degree of thermodynamic stability of metal silicides,[40] one can reasonably assume that a single crystal and powder behave in a similar way when exposed to the electron beam during the measurement.
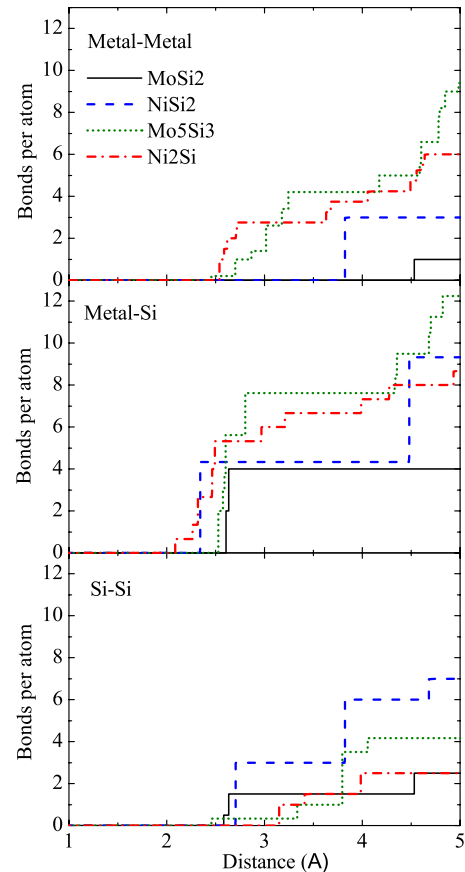

FIG. 1. (Color online) Distance dependence of the coordination number of an average atom for MoSi$_2$ (solid), NiSi$_2$ (dashed), Mo$_5$Si$_3$ (dotted), and Ni$_2$Si (dot dashed).

In XES one measures the energy dispersion of a radiative desexcitation following the creation of a core hole. The obtained spectra are proportional to the convolution of the density of the initial and final states weighted by the transition probability and by the cube of the photon energy.[41] If the desexcitation takes place from the valence band, the XES spectral density describes the response of the valence DOS to the core-hole potential, broadened by a Lorentzian function representing the DOS of the initial state (i.e., a hole in a core shell) and by a bell-shape function for the instrumental broadening. This holds only if the radiative transition probability does not vary strongly along the valence band, which is generally the case. Because of the local character of the core-hole wave function describing the initial state, and of the dipole selection rules, the observed DOS are local and partial.

In order to probe the occupied valence states of the Mo and Ni silicides, the following emission bands are analyzed:

(1) Si $L_{2,3}$ ($3s3d \rightarrow 2p$ transition), describing the Si $3s$ and $3d$ states, in the 80–100 eV photon energy range;

(2) Si $K\beta$ ($3p \rightarrow 1s$ transition), describing the Si $3p$ states, in the 1830–1850 eV photon energy range;

(3) Ni $L\alpha$ ($3d \rightarrow 2p_{3/2}$ transition), describing the Ni $3d$ states, in the 830–850 eV photon energy range;

(4) Mo $L\beta_{2,15}$ ($4d \rightarrow 2p_{3/2}$ transition), describing the Mo $4d$ states, in the 2510–2530 eV photon energy range.

All the emissions except the Si $L_{2,3}$ are collected using a high-resolution curved crystal Johann-type x-ray spectrometer.[42] In this apparatus, the working pressure is a few 10^{-7} Pa. The ionization of the samples is produced by an electron beam with an electron current density of about 1 mA/cm^2. The spectral resolution $E/\Delta E$ is 850 or better, depending on the photon energy range. The Si $L_{2,3}$ emission is obtained using a 2 m grazing incidence (1.5°) x-ray spectrometer,[43] with a 600 grooves/mm grating. The working pressure is a few 10^{-4} Pa and the electron current density is 5–10 mA/cm^2. The spectral resolution is 500. The electron-beam energy was respectively set to 1.6, 3, 4, and 6 keV for the measurement of the Ni $L\alpha$, Si $L_{2,3}$, Si $K\beta$, and Mo $L\beta$ emission bands. None of these excitation energies lies in the vicinity of an absorption edge of Si, Ni, or Mo, thereby ensuring spectra free of unwanted resonance effects. The corresponding emissive thicknesses are of the order of a few hundreds of nanometers, therefore the measurements can be considered as mostly bulk sensitive.

When compared with the theoretical DOS, the experimental DOS are set on a binding-energy scale relative to the Fermi level E_F. This is done by subtracting the binding energy of the core level involved in the transition from the photon energy scale. The Si $2p_{3/2}$ and Ni $2p_{3/2}$ binding energies are determined by XPS. The Si $1s$ binding energy is determined by combining the Si $2p_{3/2}$ binding energy and the energy of the Si $K\alpha_1$ emission ($2p_{3/2} \rightarrow 1s$ transition). The Mo $2p_{3/2}$ binding energy is determined by combining the Mo $3d_{5/2}$ binding energy, obtained by XPS, and the energy of the Mo $L\alpha_1$ emission ($3d_{5/2} \rightarrow 2p_{3/2}$ transition). Whereas for all other emissions this correction is negligible, the variation in the photon energy must be taken into account for the ultrasoft Si $L_{2,3}$ emission. Accordingly, the Si $3sd$ spectral density is divided by the cube of the photon energy.

IV. RESULTS AND DISCUSSION

A. Theoretical results

For the purpose of discussing the bonding properties, we examine the coordination numbers of an average atom plotted for the four silicides in Fig. 1. Bond lengths and numbers are found comparable for both disilicides, and very close for both metal-rich silicides. We note that the coordination numbers are higher in NiSi$_2$ than in MoSi$_2$, but in about the same proportion for the metal and Si environments. All four compounds have their first shell of nearest neighbors near 2.5 Å, where the nearest neighbors are metal-Si and Si-Si for the two disilicides, and metal-Si and metal-metal for the two metal-rich silicides. Based on these bond lengths and numbers, one may argue that the local structure in the two disilicides (metal-rich silicides) is likely to "favor" metal-Si and Si-Si (metal-Si and metal-metal) interactions. In the following discussion, changes in bonding properties between the disilicides and the metal-rich silicides will therefore be attributed to differences in the local structure. On the other hand, changes within the two disilicides, or within the two metal-rich silicides, will mainly be ascribed to differences in the spatial extent of the metal d wave function, which is known to increase with the period (i.e., in going from 3d to
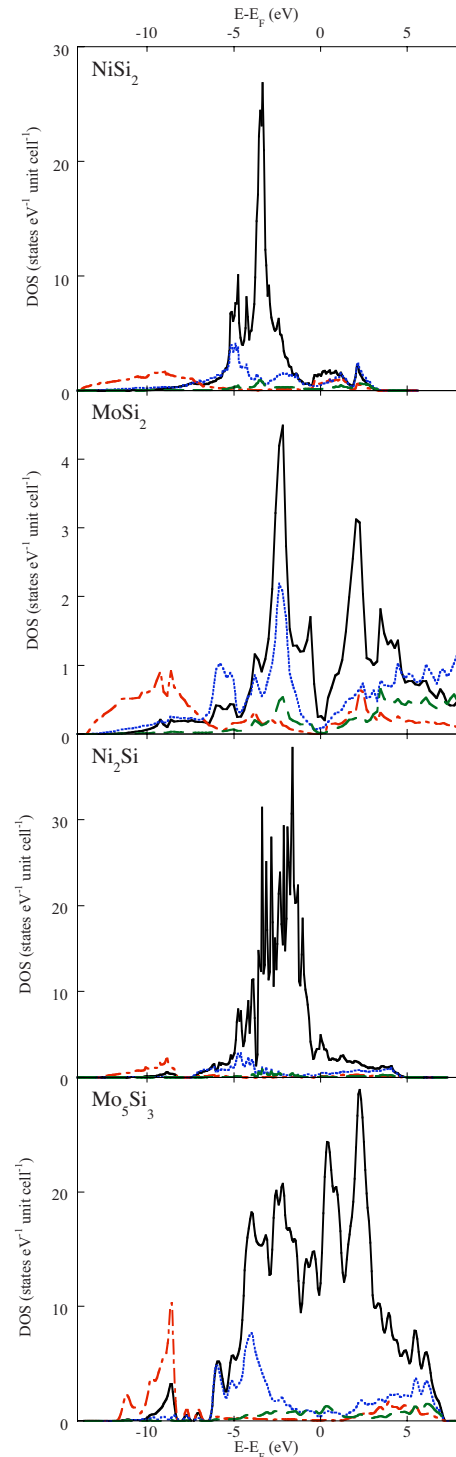

FIG. 2. (Color online) Calculated metal d (solid), Si s (dot dashed), Si p (dotted), and Si d (dashed) DOS for NiSi$_2$, MoSi$_2$, Ni$_2$Si, and Mo$_5$Si$_3$.

4d or 5d), or when the d occupancy decreases. The Mo d wave function is therefore expected to be more extended than the Ni one, resulting in an increased overlap of the Mo d states with its surroundings compared with Ni.

The projected DOS of the four compounds are presented in Fig. 2, plotted on a binding-energy scale relative to E_F. They show a good agreement with previous

studies.[5,18,20,44–46] Trends in metal silicide bonding can be inferred from close inspection of these densities. We discuss them starting from higher binding energies. The main contribution to the spectral intensity at the highest binding energy (from −14 to −7 eV) arises from the Si s states, which was previously reported to be a feature of the electronic structure of mono-, di-, and trisilicides,[11,18,20,22,29,44,47] and of metal-rich silicides but with a strongly reduced intensity.[21] Our calculations show that the compound composition affects the shape of this Si s feature rather than its intensity, as it is found much sharper for the metal-rich silicides in comparison with the disilicides, consistent with the decrease in the number of Si-Si near neighbors in the metal-rich compounds (cf. Fig. 1). On the other hand, this Si s band is distinctly stronger for the two Mo compounds and shows substantial coupling with the metal d states, contrasting with the weaker Si s feature for the Ni silicides. This is a strong indication that this Si s band is involved in the Si-metal bonding interaction, in a commensurate way with the spatial extent of the metal d orbital. This is at odds with the long-standing interpretation of this feature as being mostly nonbonding.[11,20,29] We note that this bonding interaction encompasses a finite contribution from Si p states in the disilicide case, in accord with the stronger Si-Si bonding in these compounds. On the empty-state side, some Si s states are observed to hybridize with the metal d states as well, between 0 and 5 eV.

The Si s region is followed at lower binding energy by, respectively, a crossover with Si p and metal d states for the disilicides and by a ∼1.5 eV wide gap for the metal-rich materials (quasigap for Mo_5Si_3). A substantial coupling between the Si p and metal d states resulting in a well-defined peak in the Si p DOS is centered around −5 eV for the four compounds, with virtually no Si s states. This feature is brought about by the Si-metal pd bonding interaction. Along the low binding-energy tail of this peak the electronic structure acquires a predominant d character, coinciding with a quasigap in the Si p states between the pd bonding interaction and its antibonding pendant at lower binding energies. The d states located within this quasigap participate in the metal-metal dd hybridization, they are usually called nonbonding.

It is now well established that the pd hybridization and the ensuing redistribution of the Si p states toward the bottom (pd bonding) and top (pd antibonding) of the metal d band are at the heart of silicide bonding. It follows from the literature that this interaction is determined by two main competing trends which are an increase in the bonding/antibonding splitting with the metal content[11,23,45] and a decrease in the proportion of metal d states involved in the bonding with Si with the spatial extent of the metal d wave function.[18,20,21,23] Our DOS are found consistent with this scheme, as the bonding/antibonding splitting is clearly larger for the metal-rich systems Ni_2Si (∼9 eV) and Mo_5Si_3 (∼10 eV) than for their disilicide analogs $NiSi_2$ (∼3 eV) and $MoSi_2$ (∼4 eV). Besides, whereas the narrow Ni d nonbonding states dominate the DOS of both Ni compounds, a substantial proportion of the more diffuse Mo d states is found enmeshed with the Si p states for both Mo compounds. We note that $MoSi_2$ stands as an outstanding case of strong pd hybridization, with only a very narrow region of

nonbonding d states straddling a near hybridization gap at E_F,[45] curtailed on either side by overlapping pd states.

We estimate the proportion of nonbonding metal d states for each compound by integrating the regions where there is no sizeable overlap with the Si p states (cf. energy ranges
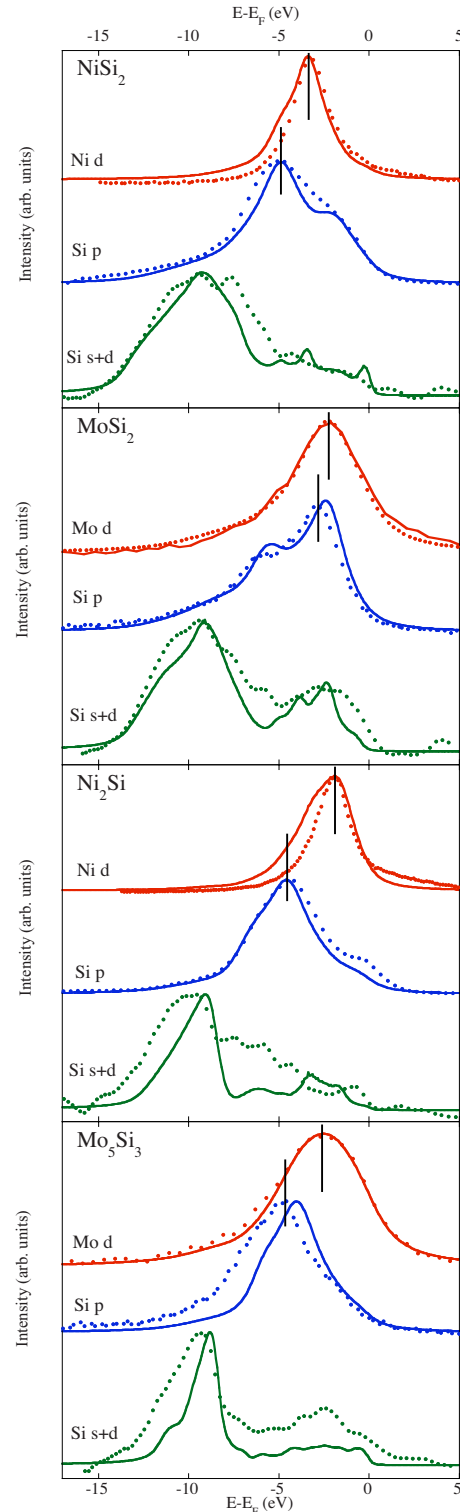

FIG. 3. (Color online) Experimental (dotted) and calculated (solid) metal d, Si p and Si $s+d$ spectra for $NiSi_2$, $MoSi_2$, Ni_2Si, and Mo_5Si_3.

into brackets): 47% for $NiSi_2$ (from -4 to -2.5 eV), 4% for $MoSi_2$ (from -1 to 0.4 eV), 72% for Ni_2Si (from -3.7 to -0.4 eV) and 39% for Mo_5Si_3 (from -2.5 to 1.5 eV). Based on these proportions, one may delineate a hierarchy in pd hybridization, from strongest to weakest: $MoSi_2$, Mo_5Si_3, $NiSi_2$, Ni_2Si. Within the uncertainty of the present estimates, the pd hybridization is found stronger in the metal-rich compound Mo_5Si_3 than in the disilicide $NiSi_2$, irrespective of the slightly shorter metal-Si bonds in $NiSi_2$ and of the stronger metal-metal interaction suggested by the local structure of Mo_5Si_3. This hierarchy indicates that the spatial extent of the metal d wave function prevails over the structure in determining the pd hybridization, hence the Si-metal bonding, in the four studied compounds.

Finally, a weak contribution from the Si d states is observed to overlap with the metal d states below E_F for the Ni compounds and both below and above E_F for the Mo compounds. The intensity of this feature is stronger for both Mo compounds, confirming the stronger Si-metal interaction in the Mo compounds in comparison with their Ni counterparts.

B. Comparison between theoretical and experimental results

Calculated and experimental DOS are presented for the four systems in Fig. 3. The agreement is good for the metal d and the Si p states, but less satisfactory for the Si sd states. We suggest that the acquisition conditions of the Si $L_{2,3}$ emission band, such as the vacuum and the current density of the incident electrons, not as good as for the other measured emissions (cf. Sec. III), could have generated slight modifications in the sample structure and/or composition. This may explain the additional structures observed in the experimental spectra compared with the calculations. Furthermore, the ratio of the transition probabilities $3d \rightarrow 2p_{3/2}/3s \rightarrow 2p_{3/2}$, unknown, is taken as 1. One may obtain a better agreement with the calculated spectra if using a higher ratio for the metal-rich materials.

We observe that the calculated Ni d spectra are broader than the experimental ones on the high-energy side for both Ni compounds. This is a signature of strong dd correlations typical of nearly fully filled $3d$ band transition metals, which are not properly accounted for in the present calculations. Similar discrepancies between experimental and theoretical data have been previously reported for other Ni compounds.[48,49] The difference is more pronounced for Ni_2Si compared to $NiSi_2$, reflecting the fact that the d states in Ni_2Si have a stronger Ni metal-like character,[46] hence a higher sensitivity to the final-state effect than in $NiSi_2$.

We examine now the emission spectra and discuss the bonding properties along the lines of Sec. IV A. Starting with the Si $L_{2,3}$ band, the main peak near -10 eV is expected to reflect the Si s states. It is found narrower for the

two metal-rich compounds compared with the disilicides, which agrees well with the calculated Si s bands and is consistent with the diminished Si-Si bonding component in the metal-rich systems. Toward lower binding energies the experimental spectrum gains gradually intensity from the $3d \rightarrow 2p_{3/2}$ transition, and the peak centered near -2.5 eV is expected to describe the Si d states. This peak, overlapping with the metal L emission band, is observed to be stronger for the Mo compounds than for the Ni compounds. This is congruent with the stronger Si-metal dd overlap observed for the Mo compounds in the calculated DOS (cf. Fig. 2).

A striking difference between $MoSi_2$ and the other compounds is observed in the respective positions of the Si $K\beta$ and metal L bands, which describe, respectively, the Si p and metal d states. The two bands are found to strongly overlap in the $MoSi_2$ case, as seen from their respective maximum coinciding around -2.5 eV. The maximum of the metal L band is observed to lie in between the main peak (~-5 eV) and the low binding-energy shoulder (~-1 eV) of the Si $K\beta$ band for the other silicides, signifying a substantially weaker pd overlap. We observe that the Ni $L\alpha$ band is narrower than the Mo $L\beta_{2,15}$ band, consistent with the more diffuse character of the Mo d states. Overall, these spectra provide a valuable experimental confirmation of the bonding trends inferred from the calculated DOS.

V. CONCLUSION

We have studied the bulk electronic structure of the silicides $NiSi_2$, Ni_2Si, $MoSi_2$, and Mo_5Si_3 using a combination of XES and density functional theory. Good agreement is obtained between the calculated and experimental local and partial DOS. The main features of both calculated and experimental spectra are pinpointed and assigned to specific bonding mechanisms. The coupling between the Si and metal states is observed to come about through the sequence sd-pd-dd from high to low binding energy, followed by a region of metal d nonbonding states at lower binding energy. Based on an evaluation of the proportion of nonbonding states for each compound, we suggest a hierarchy in pd hybridization strength: $MoSi_2 > Mo_5Si_3 > NiSi_2 > Ni_2Si$. This suggests that the chemical bonding in silicides is mainly the result of two competing trends, the extension of the metal d wave function, and the local structure. The former trend is here dominant as seen from the stronger pd hybridization in Mo_5Si_3 compared with $NiSi_2$.

*Present address: Synchrotron Radiation Research Unit, Japan Atomic Energy Agency, 1-1-1 Kouto, Sayo, Hyogo 679-5148, Japan; jarrige@spring8.or.jp

[1] S. P. Murarka, Intermetallics **3**, 173 (1995).

[2] C. Lavoie, F. M. d'Heurle, C. Detavernier, and C. Cabral, Jr., Microelectron. Eng. **70**, 144 (2003).

[3] X.-P. Qu, Y.-L. Jiang, G.-P. Ru, F. Lu, B.-Z. Li, C. Detavernier, and R. L. Van Meirhaeghe, Thin Solid Films **462-463**, 146 (2004).

[4] C. M. Liu, W. L. Liu, S. H. Hsieh, T. K. Tsai, and W. J. Chen, Appl. Surf. Sci. **243**, 259 (2005).

[5] D. A. Pankhurst, Z. Yuan, D. Nguyen-Manh, M.-L. Abel, G. Shao, J. F. Watts, D. G. Pettifor, and P. Tsakiropoulos, Phys. Rev. B **71**, 075114 (2005).

[6] J. H. Weaver, V. L. Moruzzi, and F. A. Schmidt, Phys. Rev. B **23**, 2916 (1981).

[7] Y. Imai, M. Mukaida, and T. Tsunoda, Intermetallics **8**, 381 (2000).

[8] Y. Imai, M. Mukaida, K. Kobayashi, and T. Tsunoda, Intermetallics **9**, 261 (2001).

[9] M. Ekman and V. Ozolins, Phys. Rev. B **57**, 4419 (1998).

[10] M. Taguchi, F. Le Normand, J. Hommet, S. Rey, G. Schmerber, and J.-C. Parlebas, Eur. Phys. J. B **18**, 611 (2000).

[11] O. Bisi and L. W. Chiao, Phys. Rev. B **25**, 4943 (1982).

[12] N. Franco, J. E. Klepeis, C. Bostedt, T. Van Buuren, C. Heske, O. Pankratov, T. A. Callcott, D. L. Ederer, and L. J. Terminello, Phys. Rev. B **68**, 045116 (2003).

[13] D. M. Bylander, L. Kleinman, K. Mednick, and W. R. Grise, Phys. Rev. B **26**, 6379 (1982).

[14] L. F. Mattheiss and J. C. Hensel, Phys. Rev. B **39**, 7754 (1989).

[15] A. Simunek and G. Wiech, Solid State Commun. **98**, 435 (1996).

[16] C. L. Fu, X. Wang, Y. Y. Ye, and K. M. Ho, Intermetallics **7**, 179 (1999).

[17] S. I. Kurganskii, N. S. Pereslavtseva, E. V. Levitskaya, and Yu. A. Yurakov, Phys. Status Solidi B **233**, 306 (2002).

[18] T. Shaoping and Z. Kaiming, J. Phys. C **21**, 1469 (1988).

[19] Y. J. Chabal, D. R. Hamann, J. E. Rowe, and M. Schluter, Phys. Rev. B **25**, 7598 (1982).

[20] W. Speier, E. v. Leuken, J. C. Fuggle, D. D. Sarma, L. Kumar, B. Dauth, and K. H. J. Buschow, Phys. Rev. B **39**, 6008 (1989).

[21] W. Speier, L. Kumar, D. D. Sarma, R. A. de Groot, and J. C. Fuggle, J. Phys.: Condens. Matter **1**, 9117 (1989).

[22] J. H. Weaver, A. Franciosi, and V. L. Moruzzi, Phys. Rev. B **29**, 3293 (1984).

[23] A. Franciosi, J. H. Weaver, and F. A. Schmidt, Phys. Rev. B **26**, 546 (1982).

[24] A. Franciosi, J. H. Weaver, D. G. O'Neill, F. A. Schmidt, O. Bisi, and C. Calandra, Phys. Rev. B **28**, 7000 (1983).

[25] F. Vergand, P. Jonnard, and C. Bonnelle, Europhys. Lett. **10**, 67 (1989).

[26] M. Kefi, P. Jonnard, F. Vergand, C. Bonnelle, and E. Gillet, J. Phys.: Condens. Matter **5**, 8629 (1993).

[27] P. Jonnard, F. Vergand, C. Bonnelle, E. Orgaz, and M. Gupta, Phys. Rev. B **57**, 12111 (1998).

[28] P. Jonnard, N. Capron, F. Semond, J. Massies, E. Martinez-Guerrero, and H. Mariette, Eur. Phys. J. B **42**, 351 (2004).

[29] P. J. W. Weijs, H. van Leuken, R. A. de Groot, J. C. Fuggle, S. Reiter, G. Wiech, and K. H. J. Buschow, Phys. Rev. B **44**, 8195 (1991).

[30] S. I. Kurganskii, N. S. Pereslavtseva, E. V. Levitskaya, Y. A. Yurakov, I. G. Rudneva, and E. P. Domashevskaya, J. Phys.: Condens. Matter **14**, 6833 (2002).

[31] G. Kresse and J. Hafner, Phys. Rev. B **49**, 14251 (1994).

[32] G. Kresse and J. Furthmüller, Comput. Mater. Sci. **6**, 15 (1996).

[33] M. Krajčí and J. Hafner, J. Phys.: Condens. Matter **14**, 5755 (2002).

[34] M. Krajčí and J. Hafner, J. Phys.: Condens. Matter **14**, 7201 (2002).

[35] P. Raybaud, J. Hafner, G. Kresse, and H. Toulhoat, J. Phys.: Condens. Matter **9**, 11107 (1997).

[36] G. Kresse and D. Joubert, Phys. Rev. B **59**, 1758 (1999).

[37] H. J. Monkhorst and J. D. Pack, Phys. Rev. B **13**, 5188 (1976).

[38] J. P. Perdew, J. A. Chevary, S. H. Vosko, K. A. Jackson, M. R. Pederson, D. J. Singh, and C. Fiolhais, Phys. Rev. B **46**, 6671 (1992).

[39] P. Villars and L. D. Calvert, *Pearson's Handbook of Crystallographic Data for Intermetallic Phases*, 2nd ed. (ASM International, Materials Park, Ohio, 1991).

[40] R. D. Weir, Pure Appl. Chem. **71**, 1215 (1999).

[41] C. Bonnelle, Annu. Rep. Prog. Chem., Sect. C: Phys. Chem. **84**, 201 (1987).

[42] C. Bonnelle, F. Vergand, P. Jonnard, J.-M. André, P.-F. Staub, P. Avila, P. Chargelègue, M.-F. Fontaine, D. Laporte, P. Paquier, A. Ringuenet, and B. Rodriguez, Rev. Sci. Instrum. **65**, 3466 (1994).

[43] J. L. Schwob, A. W. Wouters, S. Suckewer, and M. Finkenthal, Rev. Sci. Instrum. **58**, 1601 (1987).

[44] J. Tersoff and D. R. Hamann, Phys. Rev. B **28**, 1168 (1983).

[45] A. K. McMahan, J. E. Klepeis, M. van Schilfgaarde, and M. Methfessel, Phys. Rev. B **50**, 10742 (1994).

[46] O. Bisi and C. Calandra, J. Phys. C **14**, 5479 (1981).

[47] K. A. Mäder, H. von Känel, and A. Baldereschi, Phys. Rev. B **48**, 4364 (1993).

[48] M. C. Desjonqueres and F. Cyrotlackmann, J. Phys. F: Met. Phys. **5**, 1368 (1975).

[49] P. J. Durham, J. Phys. F: Met. Phys. **12**, 1539 (1982).